Journal of Physiology - Paris xxx (2011) xxx–xxx

Contents lists available at SciVerse ScienceDirect

Journal of Physiology - Paris

journal homepage: www.elsevier.com/locate/jphysparis

Synthesizing complex movement fragment representations from motor cortical ensembles

Nicholas G. Hatsopoulos [a,c,*], Yali Amit [b,c]

[a] Dept. of Organismal Biology and Anatomy, University of Chicago, Chicago, IL 60637, United States
[b] Dept. of Statistics, University of Chicago, Chicago, IL 60637, United States
[c] Committee on Computational Neuroscience, University of Chicago, Chicago, IL 60637, United States

ARTICLE INFO

Article history:
Available online xxxx

Keywords:
Motor cortex
Synchrony
Trajectory encoding
Generalized linear modeling
Neural ensembles

ABSTRACT

We have previously shown that the responses of primary motor cortical neurons are more accurately predicted if one assumes that individual neurons encode temporally-extensive movement fragments or preferred trajectories instead of static movement parameters (Hatsopoulos et al., 2007). Building on these findings, we examine here how these preferred trajectories can be combined to generate a rich variety of preferred movement trajectories when neurons fire simultaneously. Specifically, we used a generalized linear model to fit each neuron's spike rate to an exponential function of the inner product between the actual movement trajectory and the preferred trajectory; then, assuming conditional independence, when two neurons fire simultaneously their spiking probabilities multiply implying that their preferred trajectories add. We used a similar exponential model to fit the probability of simultaneous firing and found that the majority of neuron pairs did combine their preferred trajectories using a simple additive rule. Moreover, a minority of neuron pairs that engaged in significant synchronization combined their preferred trajectories through a small scaling adjustment to the additive rule in the exponent, while preserving the shape of the predicted trajectory representation from the additive rule. These results suggest that complex movement representations can be synthesized in simultaneously firing neuronal ensembles by adding the trajectory representations of the constituents in the ensemble.

1. Introduction

At the beginning of the 20th century, Sherrington proposed that the motor cortex was the site where complex motor actions were synthesized (Leyton and Sherrington, 1917). According to this proposal, individual motor cortical neurons represent elementary motor actions, and complex movements are synthesized by the coordinated activations of multiple motor cortical neurons which are mediated by the extensive anatomical connectivity among these neurons (Huntley and Jones, 1991; Keller, 1993). This is very different than the contemporary viewpoint that motor cortical neurons encode abstract movement parameters such as position, velocity, direction, or force (Evarts, 1968; Smith et al., 1975; Hepp-Reymond et al., 1978; Georgopoulos et al., 1982, 1984; Moran and Schwartz, 1999; Paninski et al., 2004). However, we have recently provided evidence that the encoding properties of single primary motor cortical neurons (MI) are more accurately characterized as temporally-extensive movement trajectories which is reminiscent of the original Sherringtonian view of motor cortical encoding. In particular, we have shown that MI neurons possess preferred movement trajectories that extend several hundred milliseconds in duration. By temporally integrating these preferred trajectories, we find that individual neurons encode fragments of movement (termed "pathlets") that possess unique spatiotemporal shapes. Pathlet representations have been experimentally demonstrated during constrained two-dimensional reaching movements and, more recently, during grasping movements (Hatsopoulos et al., 2007; Saleh et al., 2010).

In this work, we sought to test the second part of Sherrington's proposal by showing how the co-activation of multiple MI neurons in an ensemble represent movement trajectories which are synthesized from the movement fragments represented by the constituent neurons in the ensemble. In particular, in the vast majority of cases, the simultaneous firing of two MI neurons encodes a preferred movement trajectory which is the linear sum of the preferred trajectories of each of the neurons in the pair which we term the "additive rule". Moreover, we show that a scaled version of the additive rule applies to neuronal pairs that engage in significant synchronization.

* Corresponding author. Address: Dept. of Organismal Biology & Anatomy, 1027 East 57th Street, Chicago, IL 60637, United States. Tel.: +1 773 702 5594; fax: +1 773 702 0037.
E-mail address: nicho@uchicago.edu (N.G. Hatsopoulos).

0928-4257/$ - see front matter © 2011 Elsevier Ltd. All rights reserved.
doi:10.1016/j.jphysparis.2011.09.003

Please cite this article in press as: Hatsopoulos, N.G., Amit, Y. Synthesizing complex movement fragment representations from motor cortical ensembles. J. Physiol. (2011), doi:10.1016/j.jphysparis.2011.09.003

2. Methods

2.1. Behavioral task

Three macaque monkeys (*Macaca mulatta*) were operantly trained to perform a random-sequence task (RS) by moving a cursor to targets via contralateral arm movements (Fig. 1A). A sequence of seven targets appeared on the projection surface. At any one time, a single target appeared at a random location in the workspace, and the monkey was required to move to it. As soon as the cursor reached the target, the target disappeared and a new target appeared in a new, random location. After reaching the 7th target, the monkey was rewarded with a drop of water. The task involved projecting the cursor and targets onto a horizontal, reflective surface in front of the monkey above the monkey's hand. The monkey's arm rested on cushioned arm troughs secured to links of a two-joint robotic arm (BKIN Technologies, ON, Canada, (Scott, 1999) underneath the projection surface. The shoulder joint was abducted 90 degrees such that shoulder and elbow flexion and extension movements were made in the horizontal plane. The shoulder and elbow joint angles were sampled at 500 Hz by the robotic arm's motor encoders. The x and y positions of the hand were computed using the forward kinematics equations.

2.2. Electrophysiology

A silicon-based electrode array composed of 100 electrodes (1.0 mm electrode length; 400 μm inter-electrode separation) was implanted in the arm area of primary motor cortex (MI) of each monkey. During a recording session, signals from up to 96 electrodes were amplified (gain, 150) and recorded digitally (14-bit) at 30 kHz per channel using a Cerebus acquisition system (BlackRock Microsystems, Inc., UT). Only waveforms (1.6 ms in duration) that crossed a threshold were stored and spike-sorted using Offline Sorter (Plexon, Inc., Dallas, TX). Inter-spike interval histograms were computed to verify single-unit isolation. Signal-to-noise ratios were defined as the difference in mean peak-to-trough voltage divided by twice the standard deviation. All isolated single units used in this study possessed signal-to-noise ratios of 4:1 or higher. A total of three data sets, one from each animal were analyzed, where a data set is defined as all simultaneously recorded units collected in one recording session. Because we examined simultaneous firing between pairs of neurons, we considered only units whose average firing rate was greater than 1 Hz throughout the experiment to ensure that there were adequate numbers of simultaneous events to improve the likelihood that the generalized linear model would converge (see Section 2.3). Each data set contained 44, 17, and 87 simultaneously recorded units from MI with an average firing rate greater than 1 Hz from monkey R, B, and RS, respectively. Neural ensembles consisted of "randomly" selected units from MI except for a possible bias for neurons with large cell bodies that would generate higher signal-to-noise ratios. All of the surgical and behavioral procedures were approved by the University of Chicago's IACUC and conform to the principles outlined in the Guide for the Care and Use of Laboratory Animals (NIH publication no. 86–23, revised 1985).

2.3. Encoding model

We employed a generalized linear model with a log link function and assumed Poisson noise to fit an exponential relationship between the expected value of the spike count (within a small time interval) and the velocity trajectory of the hand, $\vec{v}^t$:

$$E(count(t)|\vec{v}^t) = \exp[\vec{k}\cdot\vec{v}^t + \gamma] \approx P(spike(t)|\vec{v}^t) \quad (1)$$

Since the sampling time interval is small (i.e. 10 ms) we can assume that the mean spike count is approximately equal to the probability of a spike occurring in that interval. The exponential (i.e. log link function) is a standard statistical relationship used when the dependent variable is a count random variable that is Poisson distributed (McCullagh and Nelder, 1989). This function ensures that the dependent variable is not negative. The vector $\vec{k}$ is called the preferred trajectory of the neuron and γ is an offset parameter of the model. Each velocity trajectory extends over a range of times before and after the measured spike count time t:

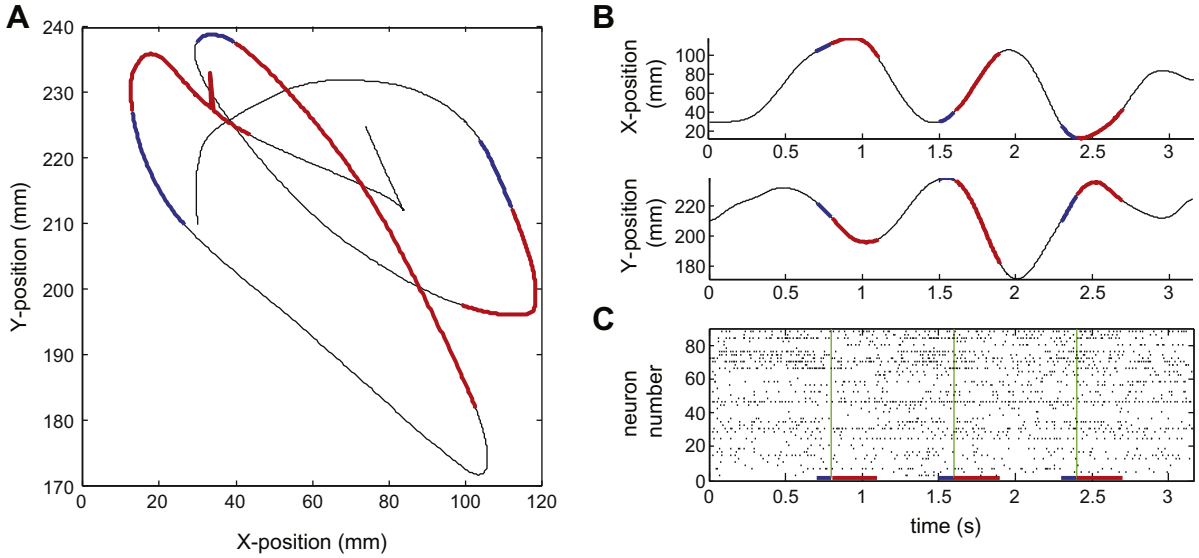

Fig. 1. Behavioral task and sampling methodology. (A) Example of a single successful behavioral trial in the random-sequence task. The targets are not presented for clarity. Three sample paths (blue and red segments) are also shown which were used to build the exponential encoding model. These samples are separated by 800 ms for clarity in the figure whereas sampling was done every 50 ms to build the model. (B) The x- and y-trajectories of the hand are shown as well as the three sample trajectories associated with the sample paths in A. (C) Raster plots from a group of simultaneously recorded neurons along with the durations of the trajectory samples (blue and red horizontal lines) and the spike sampling times (green vertical lines) associated with each trajectory sample.

Please cite this article in press as: Hatsopoulos, N.G., Amit, Y. Synthesizing complex movement fragment representations from motor cortical ensembles. J. Physiol. (2011), doi:10.1016/j.jphysparis.2011.09.003

$$\vec{v}^t \equiv (v_x(t-100\text{ ms}),\ldots,v_x(t+n\Delta t),\ldots,v_x(t+300\text{ ms}),v_y(t-100\text{ ms}),\ldots,v_y(t+n\Delta t),\ldots,v_y(t+300\text{ ms}))$$

where $v_x(t+n\Delta t)$ and $v_y(t+n\Delta t)$ are the x- and y-components of the hand velocity respectively, at time $t+n\Delta t$ where $\Delta t = 2$ ms. We have previously shown that the optimal velocity trajectory (in terms of predicting neural responses) was asymmetric such that it extended 100 ms in the past and 300 ms in the future with respect to time t (Hatsopoulos et al., 2007). Therefore, in this work n is an integer ranging from −50 to +150. We chose a velocity trajectory as opposed to a position trajectory representation because previous research has indicated that motor cortical activity correlates more strongly with velocity (i.e. direction and speed) than with position (Ashe and Georgopoulos, 1994).

We modified the basic encoding model in Eq. (1) in the following way. The velocity trajectories were divided by their L2-norm to create the normalized velocity trajectories: $\hat{v}^t = \frac{\vec{v}^t}{\|\vec{v}^t\|}$. Normalization captures the pattern of variation in the velocity (i.e. direction and relative speed) over time but ignores overall speed which is known to influence the firing of motor cortical neurons (Moran and Schwartz, 1999). In addition, it has been observed that static and dynamic position weakly affects motor cortical activity (Georgopoulos et al., 1984; Paninski et al., 2004). Therefore, covariates in the model included terms reflecting the average speed, $\bar{v}^t$, and position, $(\bar{x}^t,\bar{y}^t)$, of the trajectory:

$$P(spike(t)|\hat{v}^t,\bar{v}^t,\bar{x}^t,\bar{y}^t) = \exp[\vec{k}\cdot\hat{v}^t + a\bar{v}^t + b\bar{x}^t + c\bar{y}^t + \gamma] \quad (2)$$

where as above, $\vec{k}$ is referred to as the *preferred velocity trajectory* of the neuron since the inner product in the exponent is maximized when the $\hat{v}^t$ vector is aligned with it. The preferred path or *pathlet* of the neuron is obtained by integrating $\vec{k}$ in time as if it were a vector of velocities. Although the pathlet representation is the integral of velocity, it is not tied to specific positions in the workspace but rather characterizes the temporal dynamics of velocity encoding. To estimate the coefficients in the model, multiple velocity trajectories were sampled by extracting position trajectories (x- and y-trajectories sampled every 2 ms) every 50 ms throughout successfully completed trials of the RS task resulting in tens of thousands of sample trajectories in a typical data set (Fig. 1B). These position trajectories were smoothed by replacing each sample point with the time averaged position (±50 ms about the sample point), and then numerically differentiated to generate a set of velocity trajectory samples. Trajectories with peak velocities greater than 100 cm/s were excluded from the model. For each sample velocity trajectory, we associated a spike sampling time and interval (10 ms duration) and measured the spike count in that interval (Fig. 1C). Because the interval was so short, we typically observed no spikes or one spike. In the rare cases with more than one spike occurring in a 10 ms interval, we considered it as a single spike event. Therefore, the neural response was binary.

To reduce the dimensionality of $\vec{v}^t$ (e.g. 600 dimensional for a 600 ms trajectory length; 300 dimensions for x and y, respectively) we performed a principal component analysis on all sample velocity trajectories (prior to normalization). The first 10 principal components accounted for over 90% of the variance so we assumed that $\vec{k}$ is a linear combination of these top 10 components, i.e. $\vec{k} = U\vec{\beta}$, where $\vec{\beta}$ is a 10 dimensional parameter vector (referred to as the *transformed preferred velocity trajectory*) and U is a matrix of 10 columns each corresponding to a principal component. The 14 free parameters, $\vec{\beta}$ (10 dimensional), a, b, c, γ were estimated by maximum likelihood using standard methods for generalized linear models (glmfit function in Matlab). The exponent in Eq. (2) is denoted the *linear predictor*. When comparing the exponential model to the data, we computed the linear predictor for each sample trajectory. This set of scalar values was then ordered and divided into equal sized quantile-bins. The frequency of spikes within each bin was computed and shown as a blue point in a graph of the probability versus linear predictor.

2.4. Joint spiking analysis

For the joint spiking of a pair of neurons assuming conditional independence we get the *additive joint model*:

$$\begin{aligned} P(spike_1(t)\wedge spike_2(t)|\hat{v}_t) &= \exp[\vec{k}_1\cdot\hat{v}^t + a_1\bar{v}^t + b_1\bar{x}^t + c_1\bar{y}^t \\ &\quad + \gamma_1]\cdot\exp[\vec{k}_2\cdot\hat{v}^t + a_2\bar{v}^t + b_2\bar{x}^t \\ &\quad + c_2\bar{y}^t + \gamma_2] \\ &= \exp[(\vec{k}_1 + \vec{k}_2)\cdot\hat{v}^t + (a_1+a_2)\bar{v}^t \\ &\quad + (b_1+b_2)\bar{x}^t + (c_1+c_2)\bar{y}^t + (\gamma_1 \\ &\quad + \gamma_2)] \end{aligned} \quad (3)$$

The additive model is compared to the *fitted joint model*

$$P(spike_1(t)\wedge spike_2(t)|\hat{v}^t) = \exp[\vec{k}_{12}\cdot\hat{v}^t + a_{12}\bar{v}^t + b_{12}\bar{x}^t + c_{12}\bar{y}^t + \gamma_{12}] \quad (4)$$

$\vec{k}_1 + \vec{k}_2 = U(\vec{\beta}_1 + \vec{\beta}_2)$ is then the additive joint preferred velocity trajectory and its integral is the additive preferred pathlet, and $\vec{k}_{12} = U\vec{\beta}_{12}$ is the fitted joint preferred velocity trajectory and its integral is the fitted joint preferred pathlet. $\vec{\beta}_1 + \vec{\beta}_2, \vec{\beta}_{12}$ are the transformed additive and fitted preferred trajectories, respectively. These two preferred trajectories for pairs of neurons are compared.

2.5. Receiver-operating characteristic curves

In order to assess the degree to which the encoding model fit the data, receiver-operating-characteristic (ROC) curves were generated to quantify the relationship between the probability of correctly predicting a spike (hit probability) versus the probability of incorrectly predicting a spike when it was absent (false-positive probability). The curve was generated by systematically varying a threshold for predicting a spike. For each threshold value, a spike was assumed to occur if the spiking probability, as computed by the model, exceeded the threshold. To verify that the model was not over-fitting the data, all ROC analyses were performed on test data that were not used to estimate the model parameters. We assigned a random 90% of the data (i.e. training data) to build the encoding model, and the remaining 10% of the data was assigned as test data.

2.6. Assessing significant synchronization

The occurrence of significant synchrony was assessed by randomly and uniformly jittering each spike generated by one neuron within a time window (±20 ms) centered about the original spike time and counting the number of synchronous spikes defined as spikes in both neurons occurring within a ±5 ms of each other (Hatsopoulos et al., 2003). Significance can be assessed by repeating the jittering multiple times to create a Monte-Carlo estimation of the distribution of synchronous spikes under the null hypothesis that there is no fine temporal structure below the ±20 ms time scale. The significance is determined by the location of the unjittered synchronous count in the distribution. However, we applied a faster spike jittering algorithm which does not rely on Monte-Carlo estimation but is formally equivalent as the number of jitters approaches infinity (Algorithm courtesy of Matt Harrison). This algorithm relies on dynamic programming methods to find an exact value for the significance value (Harrison, 2005). Briefly, for each spike in the first spike train, the algorithm computed the

Please cite this article in press as: Hatsopoulos, N.G., Amit, Y. Synthesizing complex movement fragment representations from motor cortical ensembles. J. Physiol. (2011), doi:10.1016/j.jphysparis.2011.09.003

probability that it would be jittered into a position that was synchronous with a spike in the second spike train. Since spikes are jittered independently, these probabilities allow one to derive the jitter distribution of the total number of synchronous spikes using the well known convolution algorithm for the distribution of a sum of independent random variables. This is faster and more accurate than randomly jittering spikes in order to Monte Carlo approximate the jitter distribution of synchrony.

3. Results

We recorded extracellularly from multiple single units in MI using chronically implanted electrode arrays while monkeys performed a random-sequence (RS) task with their arm (see Fig. 1A). Instead of prescribing a limited set of movements, we had the animal generate a rich variety of trajectories and paths with different spatial shapes, velocities, and positions. We then applied a generalized linear model (Eq. (2)) to fit the observed spiking response for each neuron individually to an exponential function of the linear predictor using maximum likelihood estimation (Fig. 2A, left panel). The fitted model provided an estimate of the preferred velocity trajectories (Fig. 2A, middle panel). By integrating the preferred velocity trajectory, we determined the preferred path or pathlet for each neuron (Fig. 2A, right panel). Our previous work demonstrated that an encoding model with velocity trajectories that extended 400 ms in duration (100 ms prior to the measured neural response to 300 ms following the neural response) maximized the predictive power of the model (Hatsopoulos et al., 2007). Therefore, we applied the same trajectory duration to fit each neuron's response. The model was fit to a random 90% of the data and then its predictive power was assessed on the remaining 10% of the data using ROC analysis (see Section 2) (Fig. 2B, left panel). The area under the ROC curve can range from 0.5 (chance performance) to 1 (perfect prediction). Over all 148 MI neurons analyzed, we observed a range of ROC areas with a mean (standard deviation) value of 0.62 (0.07) (Fig. 2B, right panel). A rich variety of pathlet representations are observed across a simultaneously recorded ensemble of motor cortical neurons (Fig. 3).

We then sought to predict how pairs of neurons firing simultaneously could represent more complex movement primitives by combining their preferred trajectories or pathlets. Assuming that, conditional on the movement trajectory, the firing probabilities of the two neurons at any given time instance are statistically independent, the probabilities multiply. Due to the exponential nature of the encoding model, the linear predictors (i.e. the exponents) are summed. We refer to this as the additive rule (see Eq. (3)), which implies that the preferred trajectory (and pathlet) of the neuron pair is the sum of the two constituent neurons' preferred trajectories (and pathlets).

There is, however, considerable evidence from recordings throughout cortex including motor cortex that certain neurons engage in significant synchronization, which calls into question the assumption of conditional independence in certain cases (Murphy et al., 1985; Smith and Fetz, 1989; Hatsopoulos et al., 1998; Baker et al., 2001; Jackson et al., 2003). Cross-correlation analysis revealed sharp peaks centered at zero time lag among a subset of neuron pairs which was suggestive of fine temporal synchrony. To quantify the degree and prevalence of significant synchronization, we applied a spike-jittering procedure which can uncover excessive synchronization between pairs of neurons (Hatsopoulos et al., 2003). We applied a faster algorithm to perform the spike jittering procedure that does not rely on a Monte-Carlo estimation on

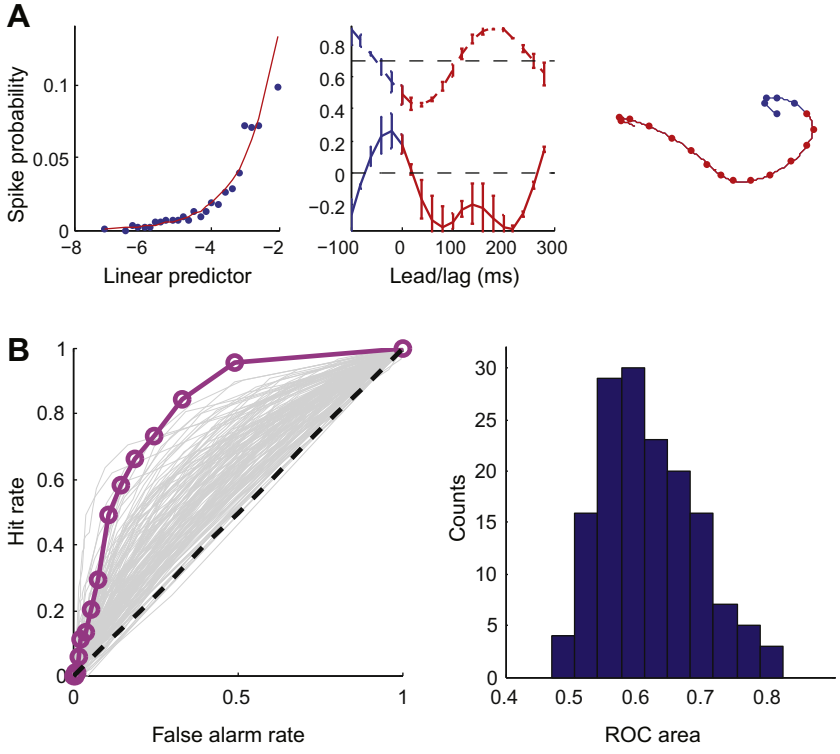

Fig. 2. The trajectory encoding model. (A) (Left panel) The fitted model probability of a spike occurring in the spike sampling window (red line) as well as the empirical spiking probability (blue points) for one MI neuron as a function of the linear predictor. The linear predictor is the value of the exponent in the model (Eq. (2)). (Middle panel) The preferred x-trajectory (below) and y-trajectory for the neuron fit with the encoding model determined from $\vec{k}$. (Right panel) The preferred path or "pathlet" of the neuron generated by temporally integrating the fitted $\vec{k}$. The blue portion of the pathlet occurs prior to the spike sampling time whereas the red portion occurs after the spike sampling time. (B) (Left panel) A receiver-operating characteristic (ROC) curve for the encoding model of the MI neuron shown in (A) (pink curve) as well as ROC curves for all recorded neurons (gray curves). (Right panel) The distribution of ROC areas for all recorded MI neurons.

Please cite this article in press as: Hatsopoulos, N.G., Amit, Y. Synthesizing complex movement fragment representations from motor cortical ensembles. J. Physiol. (2011), doi:10.1016/j.jphysparis.2011.09.003

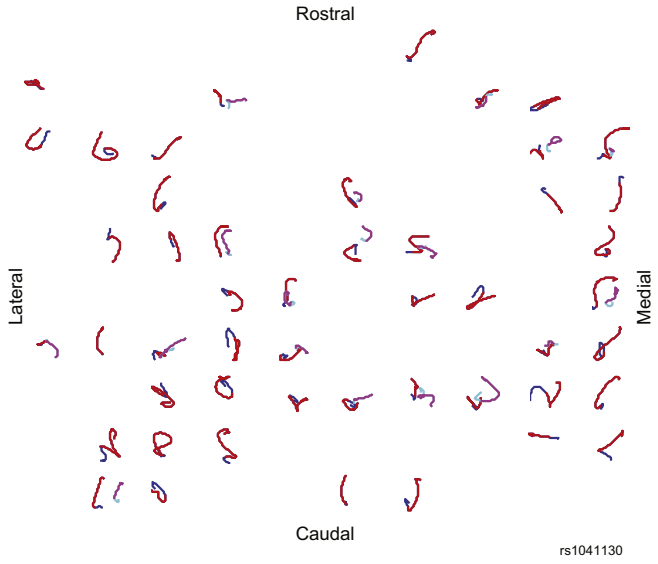

Fig. 3. A map of pathlet representations across a set of simultaneously recorded units in primary motor cortex. The relative position of each pathlet corresponds to the relative position of the electrode on which the unit was recorded on the array. Pathlets associated with a second unit recorded on the same electrode are shown in cyan and magenta. Some electrodes captured more than two units but their pathlets are not shown for clarity. Only pathlets associated with models whose ROC areas were greater than 0.55 are shown.

all cell pairs (Harrison, 2005). Among all 4823 MI cell pairs from all three data sets, 7.7% (386/4823) engaged in significant synchronization at the $p < 0.05$ level: 12% (112/946) from animal R, 6.7% (9/136) from animal B, and 6.7% (248/3741) from animal RS.

We first verified that the additive rule applied to those cell pairs that did not exhibit significant synchronization. We compared the additive joint model to the actual fitted joint model generated by fitting the exponential model to the simultaneous firing of the two neurons (see Section 2). As an example, we considered two non-synchronized neurons and generated pathlets for each of them individually (Fig. 4A, first and second panels). We then built a fitted joint model for the simultaneous firing of neurons 1 and 2 using Eq. (4) (Fig. 4A, third panel). Despite the fact that the additive joint model has no additional free parameters, it fit the simultaneous firing of the neuron pair quite well (Fig. 4A, fourth panel). Moreover, the fitted joint pathlet (Fig. 4A, third panel inset) resembles the sum of the two neuron's pathlets quite closely (Fig. 4A, fourth panel inset). We fit a joint model for the simultaneous firing of two other non-synchronized neurons and found that the additive model likewise fit the data quite well and the fitted joint pathlet closely matched the sum of the constituent neurons' pathlets (Fig. 4B). We fit joint models for all non-synchronized pairs of MI neuron pairs and compared the predictive power of these models to that of the additive joint models using ROC analysis (Fig. 4C). Among non-synchronized cell pairs whose fitted and additive joint models had ROC areas greater than 0.5 (948 out of 4823 pairs), there was no statistically significant difference in predictive power using the additive model as compared to the fitted model ($p = 0.37$, paired Wilcoxon signed rank test). The mean (standard deviation) difference in ROC area was 0.003 (0.036).

We then regressed the fitted joint preferred velocity trajectories, $\vec{k}_{12}$, against the sum of the preferred trajectories of the two constituent neurons in the pair, $\vec{k}_1 + \vec{k}_2$, over all non-synchronized neuron pairs in which the ROC areas for the joint fitted and additive models were greater than 0.5. Among the cell pairs with significant regressions ($p < 0.05$, 746 out of 948 cell pairs or 79%), we found that the distribution of slopes and y-intercepts was centered at one and zero, respectively, indicating a near match between the two (Fig. 4D). The mean (standard deviation) slope was 1.07 (0.28) and the mean (standard deviation) y-intercept was 0.01 (0.19).

As for the minority of cell pairs that were significantly synchronized (181 cell pairs), the additive joint model generally underestimated the simultaneous firing of cell pairs engaged in significant synchrony (Fig. 5A, red line). By plotting the log transformed joint response as a function of the linear predictor, it is evident that the additive model could be adjusted to fit the data by adding a gain factor to the linear predictor (Fig. 5B, see gray line). Therefore, we adjusted the additive joint model by adding one free parameter, a gain parameter, G, to the linear predictor to attempt to recover its predictive power:

$$\begin{aligned}&\log P(spike_1(t) \wedge spike_2(t) | \hat{v}_t) \\ &= G[(\vec{k}_1 + \vec{k}_2) \cdot \hat{v}^t + (a_1 + a_2)\bar{v}^t + (b_1 + b_2)\bar{x}^t + (c_1 + c_2)\bar{y}^t \\ &\quad + (\gamma_1 + \gamma_2)] \end{aligned} \tag{5}$$

By fitting the adjusted additive model to all cell pairs, we found that gain parameters were significantly smaller among synchronized cell pairs as compared to values for non-significantly synchronized cell pairs ($p < 0.01$, Wilcoxon rank sum test). The mean (stdev) gain values were 0.96 (0.04) and 0.99 (0.03) for synchronized versus non-synchronized neuron pairs (Fig. 5C). Consistent with this gain factor, a linear regression analysis revealed that the slopes between fitted joint and the additive joint preferred trajectories among the synchronized neuron pairs was slightly less than one, 0.99 (0.28), and was significantly smaller than the slopes for the unsynchronized neuron pairs ($p < 0.01$, Wilcoxon rank sum test). In other words, the fitted joint preferred velocity trajectory was a slightly scaled down version of the sum of the constituent neurons' preferred trajectories.

4. Discussion

We have demonstrated how the repertoire of trajectory representations can be expanded by combining the preferred trajectories of the constituent neurons in simultaneously firing neuronal pairs. For those neurons in an ensemble that fire in a conditionally independent manner, we propose a very simple additive rule by which their individual trajectory representations are combined. Among the cell pairs that we examined, the vast majority did not engage in significant synchronization. In this case, the exponential nature of the encoding model provides a principled explanation of the additive rule. This is a very powerful rule because it implies that the encoding model of a co-activating ensemble of any size consisting of statistically independent neurons is fully predicted from the models of the constituent neurons in the ensemble.

As for neural ensembles whose constituents engage in synchronized activity, we showed how the additive rule could be adjusted among neuron pairs by scaling the additive model. This implies that the preferred trajectory of a synchronized pair of neurons retains the overall shape predicted by the additive rule but is scaled down by a small factor. This suggests that a neural assembly of tightly coordinated neurons as proposed by Donald Hebb may possess an overall representation that resembles the aggregate representations of the constituents of the assembly. To provide further evidence for this hypothesis will require further work where higher-order synchronization can be measured among larger groups of neurons.

It is unclear what the functional significance of motor cortical synchronization is as it relates to the control of movement. The fact that synchronization is a relatively rare event does not imply that its effects are unreliable and not robust. Based on computer simulations, one hypothesis has been put forth which argues that muscle force can be enhanced by over 30% if a motor neuron receives

Please cite this article in press as: Hatsopoulos, N.G., Amit, Y. Synthesizing complex movement fragment representations from motor cortical ensembles. J. Physiol. (2011), doi:10.1016/j.jphysparis.2011.09.003

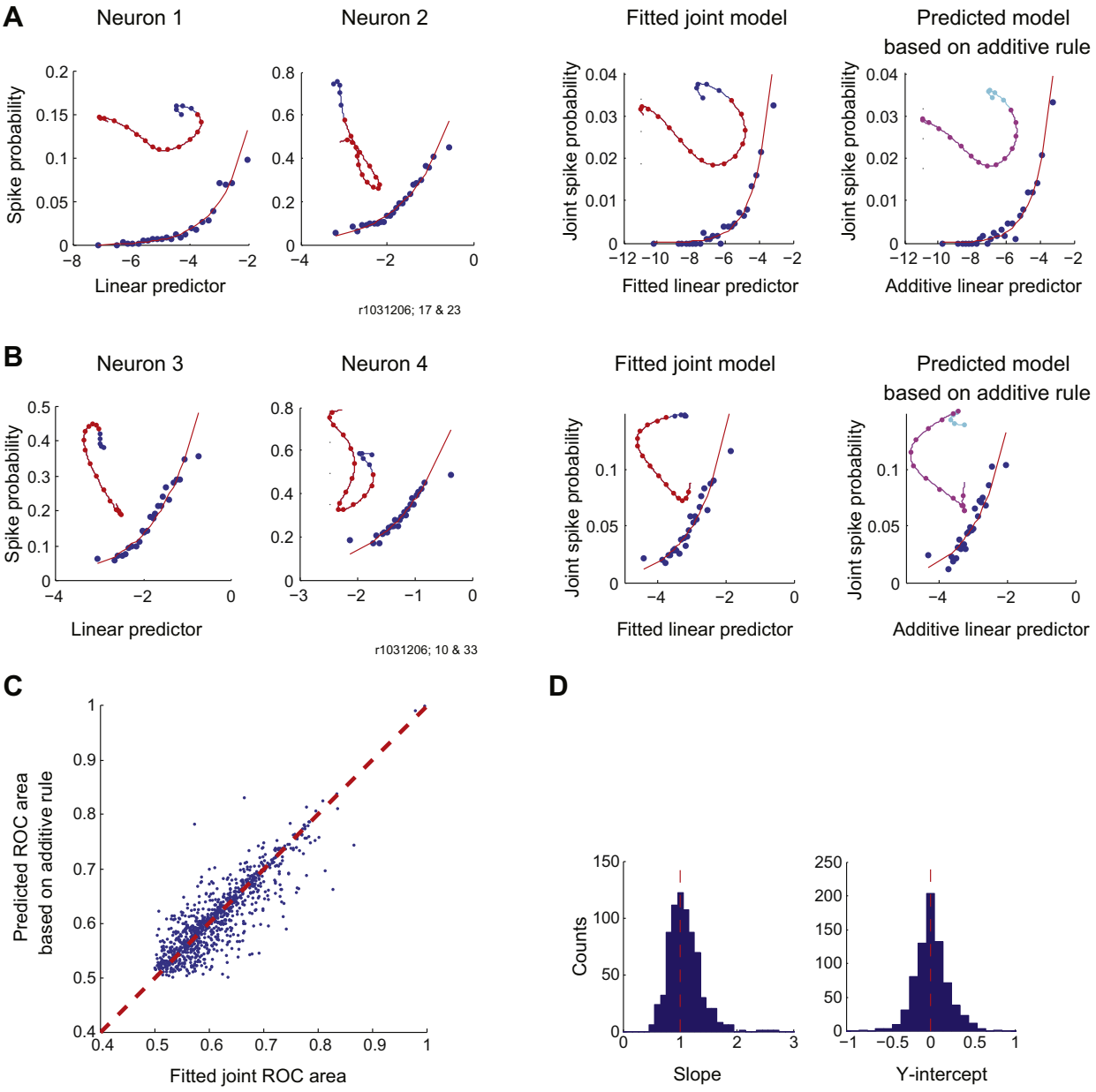

Fig. 4. Trajectory encoding of simultaneously firing neurons that are not significantly synchronized. (A) (First and second panels) The fitted model probabilities (red line) and empirical spike probabilities (blue points) for two MI neurons together with their pathlets (insets). (Third panel) The fitted joint model (red line) and empirical probabilities (blue points) for the simultaneous spiking of the two neurons as well as the estimated pathlet from the fitted joint model (inset). (Fourth panel) The predicted model based on the additive rule (red line) for the two neurons as well as the predicted pathlet. (B) Same as A. except for two other neurons. (C) A scatter plot comparing the predictive power (based on ROC area) of the additive joint model as compared to the fitted joint model. Only ROC areas that are larger than 0.5 are shown. (D) Histograms of the slopes (left panel) and y-intercepts (right panel) from a regression analysis comparing the fitted preferred velocity, $\vec{k}_{12}$, versus the sum of the preferred velocity trajectories of the constituent neurons, $\vec{k}_1 + \vec{k}_2$.

synchronized inputs (Baker et al., 1999). Another hypothesis argues that cortico-motoneuron (CM) cells are more likely to be synchronized when they project to similar groups of muscles (i.e. muscle synergies) (Jackson et al., 2003). This is based on spike-triggering of muscle (EMG) activity from CM cells which demonstrated that synchronized CM cells shared similar muscle fields as compared to CM cells that do not synchronize. Taken together, these hypotheses suggest that muscle synergies, which have been argued to be important for motor control, may be enhanced when CM cells synchronize.

The view that we have put forth in this and previous work is that individual motor cortical neurons constitute an alphabet of elementary movement fragments or primitives in a language of action. Note that we are only arguing that these complex trajectory representations more accurately capture the response variability of single motor cortical neurons. We are not claiming that these trajectory representations are inherent properties of individual motor cortical neurons independent of upstream inputs and downstream effects on the motor system. These representations are likely the consequence of both synaptic inputs onto the neurons as well as the output projections of the neurons. In particular, the negative lag time component of the fragment representation may reflect somatosensory effects on motor cortex which have been experimentally documented (Fetz et al., 1980; Suminski et al., 2010). The long duration and often complex nature of the positive lag component is more difficult to explain but may reflect persistent

Please cite this article in press as: Hatsopoulos, N.G., Amit, Y. Synthesizing complex movement fragment representations from motor cortical ensembles. J. Physiol. (2011), doi:10.1016/j.jphysparis.2011.09.003

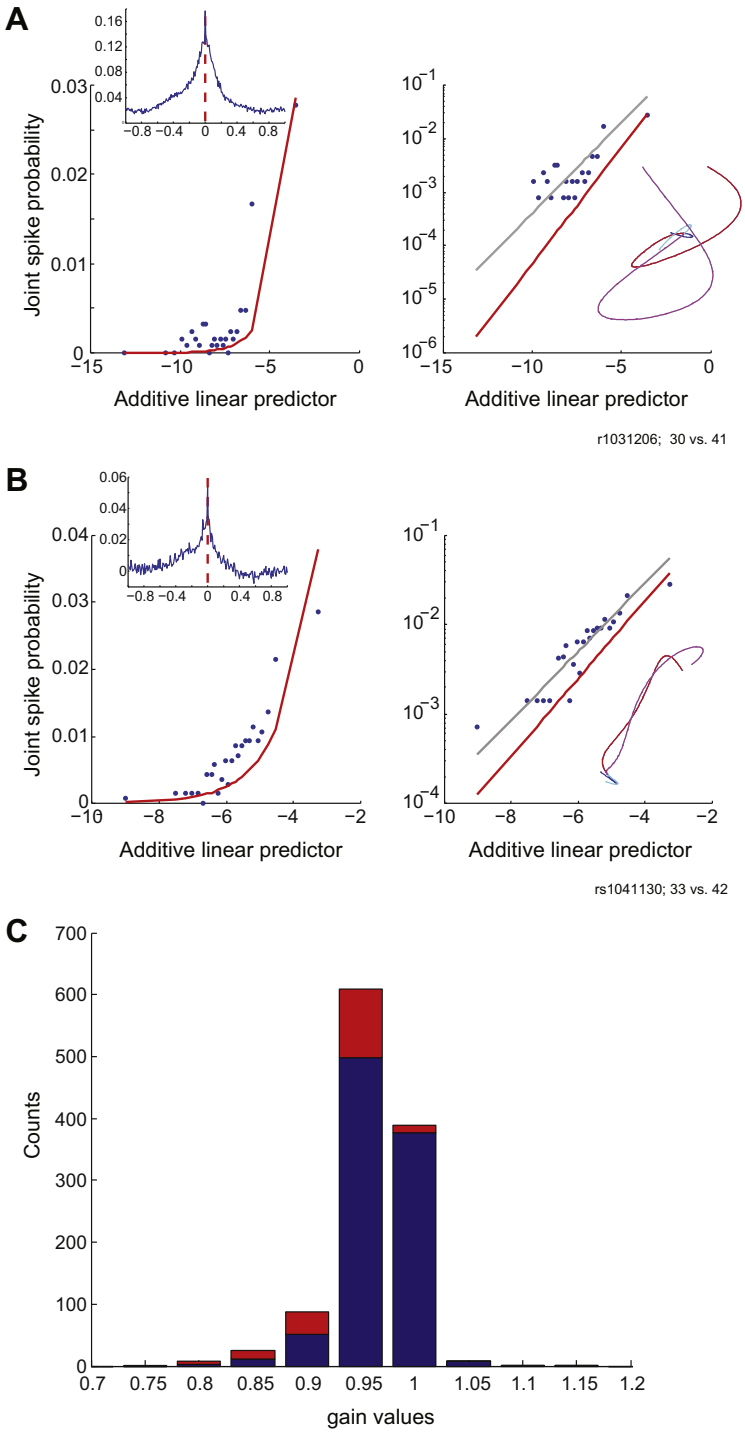

Fig. 5. Trajectory encoding among synchronized neurons. (A) (Left panel) The observed synchronous spiking probability for a pair of neurons as a function of the additive linear predictor (blue points) along with the additive model's prediction (red line). The cross-correlation (10 ms bins) from the pair of neurons is shown in the inset. (Middle panel) A log-linear transform of the left panel. The gray line is the predicted synchronous firing probability based on an additive model augmented with a gain factor. (Right panel) The fitted joint pathlet encoded by the synchronous firing of the neuron pair (blue and red lines) as well as the predicted pathlet from the additive model (cyan and magenta). (B). Same as (A) except for another pair of synchronized neurons. (C) The distribution of gain values used to augment the additive model for unsynchronized neuron pairs (blue) and synchronized pairs (red).

and complex physiological effects on downstream areas including spinal interneurons and motor neurons. For example, persistent inward currents in motor neurons have been shown to lead to temporally sustained plateau potentials that can persist even after inputs to the neuron are terminated (Lee and Heckman, 1998; Heckman et al., 2003). It has also been shown that temporally sustained and complex rhythmic whisker movements can be evoked with brief intracellular electrical stimulation of single neurons in the rat vibrissae motor cortex (Brecht et al., 2004).

If it is true that motor cortical neurons constitute an alphabet of movement fragments, the additive rule provides one syntactical principle by which these elementary primitives can be combined to form a richer set of trajectory representations when neurons fire simultaneously. Future work will investigate how these fragment

Please cite this article in press as: Hatsopoulos, N.G., Amit, Y. Synthesizing complex movement fragment representations from motor cortical ensembles. J. Physiol. (2011), doi:10.1016/j.jphysparis.2011.09.003

representations may be strung together in time when motor cortical neurons fire sequentially.

Acknowledgements

We thank Elise Covic, Adam Dickey, Matthew Fellows, Zach Haga, and Dawn Paulsen, Aaron Suminski, and Qingqing Xu for their help with the surgical implantation of the arrays, training of monkeys, data collection and analysis. This work was supported by National Institute of Neurological Disorders and Stroke Grant R01 NS045853.

References

Ashe, J., Georgopoulos, A.P., 1994. Movement parameters and neural activity in motor cortex and area 5. Cerebral Cortex 4, 590–600.

Baker, S.N., Kilner, J.M., Pinches, E.M., Lemon, R., 1999. The role of synchrony and oscillations in the motor output. Experimental Brain Research 128, 109–117.

Baker, S.N., Spinks, R., Jackson, A., Lemon, R.N., 2001. Synchronization in monkey motor cortex during a precision grip task. I. Task-dependent modulation in single-unit synchrony. Journal of Neurophysiology 85, 869–885.

Brecht, M., Schneider, M., Sakmann, B., Margrie, T.W., 2004. Whisker movements evoked by stimulation of single pyramidal cells in rat motor cortex. Nature 427, 704–710.

Evarts, E.V., 1968. Relation of pyramidal tract activity to force exerted during voluntary movement. Journal of Neurophysiology 31, 14–27.

Fetz, E.E., Finocchio, D.V., Baker, M.A., Soso, M.J., 1980. Sensory and motor responses of precentral cortex cells comparable passive and active joint movements. Journal of Neurophysiology 43, 1070–1089.

Georgopoulos, A.P., Kalaska, J.F., Caminiti, R., Massey, J.T., 1982. On the relations between the direction of two-dimensional arm movements and cell discharge in primate motor cortex. Journal of Neuroscience 2, 1527–1537.

Georgopoulos, A.P., Caminiti, R., Kalaska, J.F., 1984. Static spatial effects in motor cortex and area 5: quantitative relations in a two-dimensional space. Experimental Brain Research 54, 446–454.

Harrison, M.T., 2005. Discovering compositional structures. In: Applied Mathematics. Brown University, Providence.

Hatsopoulos, N.G., Ojakangas, C.L., Paniniski, L., Donoghue, J.P., 1998. Information about movement direction obtained from synchronous activity of motor cortical neurons. Proceedings of the National Academy of Sciences 95, 15706–15711.

Hatsopoulos, N.G., Geman, S., Amarasingham, A., Bienenstock, E., 2003. At what time scale does the nervous system operate? Neurocomputing, 25–29.

Hatsopoulos, N.G., Xu, Q., Amit, Y., 2007. Encoding of movement fragments in the motor cortex. Journal of Neuroscience 27, 5105–5114.

Heckman, C.J., Lee, R.H., Brownstone, R.M., 2003. Hyperexcitable dendrites in motoneurons and their neuromodulatory control during motor behavior. Trends in Neurosciences 26, 688–695.

Hepp-Reymond, M.-C., Wyss, U.R., Anner, R., 1978. Neuronal coding of static force in the primate motor cortex. Journal de Physiologie 74, 287–291.

Huntley, G.W., Jones, E.G., 1991. Relationship of intrinsic connections to forelimb movement representations in monkey motor cortex: a correlative anatomic and physiological study. Journal of Neurophysiology 66, 390–413.

Jackson, A., Gee, V.J., Baker, S.N., Lemon, R.N., 2003. Synchrony between neurons with similar muscle fields in monkey motor cortex. Neuron 38, 115–125.

Keller, A., 1993. Intrinsic synaptic organization of the motor cortex. Cerebral Cortex 3, 430–441.

Lee, R.H., Heckman, C.J., 1998. Bistability in spinal motoneurons in vivo: systematic variations in persistent inward currents. Journal of Neurophysiology 80, 583–593.

Leyton, S.S.F., Sherrington, C.S., 1917. Observations on the excitable cortex of the chimpanzee, orangutan and gorilla. Quarterly Journal of Experimental Physiology 11, 135–222.

McCullagh, P., Nelder, J.A., 1989. Generalized Linear Models. Chapman & Hall/CRC Press, Boca Raton, FL.

Moran, D.W., Schwartz, A.B., 1999. Motor cortical representation of speed and direction during reaching. Journal of Neurophysiology 82, 2676–2692.

Murphy, J.T., Kwan, H.C., Wong, Y.C., 1985. Cross correlation studies in primate motor cortex: synaptic interactions and shared input. Canadian Journal of Neurological Sciences 12, 11–23.

Paninski, L., Fellows, M.R., Hatsopoulos, N.G., Donoghue, J.P., 2004. Spatiotemporal tuning of motor cortical neurons for hand position and velocity. Journal of Neurophysiology 91, 515–532.

Saleh, M., Takahashi, K., Amit, Y., Hatsopoulos, N.G., 2010. Encoding of coordinated grasp trajectories in primary motor cortex. The Journal of Neuroscience: The Official Journal of the Society for Neuroscience 30, 17079–17090.

Scott, S.H., 1999. Apparatus for measuring and perturbing shoulder and elbow joint positions and torques during reaching. Journal of Neuroscience Methods 89, 119–127.

Smith, W.S., Fetz, E.E., 1989. Effects of synchrony between primate corticomotoneuronal cells on post-spike facilitation of muscles and motor units. Neuroscience Letters 96, 76–81.

Smith, A.M., Hepp-Reymond, M.C., Wyss, U.R., 1975. Relation of activity in precentral cortical neurons to force and rate of force change during isometric contractions of finger muscles. Experimental Brain Research 23, 315–332.

Suminski, A.J., Tkach, D.C., Fagg, A.H., Hatsopoulos, N.G., 2010. Incorporating feedback from multiple sensory modalities enhances brain–machine interface control. The Journal of Neuroscience: The Official Journal of the Society for Neuroscience 30, 16777–16787.

Please cite this article in press as: Hatsopoulos, N.G., Amit, Y. Synthesizing complex movement fragment representations from motor cortical ensembles. J. Physiol. (2011), doi:10.1016/j.jphysparis.2011.09.003